“Soldier–Sergeant–Soldier” Triblock Copolymers: Revealing the Folded Structure of Single-Chain Polymeric Nanoparticles

Journal:	*ChemComm*
Manuscript ID:	CC-COM-04-2014-002789.R1
Article Type:	Communication
Date Submitted by the Author:	26-May-2014
Complete List of Authors:	Meijer, E; Eindhoven University of Technology, Laboratory of Macromolecular and Organic Chemistry Palmans, Anja R. A.; TU Eindhoven, Chemistry and Chemical Engineering Hosono, Nobu; TU Eindhoven, Chemistry and Chemical Engineering

ChemComm

RSCPublishing

COMMUNICATION

“Soldier–Sergeant–Soldier” Triblock Copolymers: Revealing the Folded Structure of Single-Chain Polymeric Nanoparticles†

Cite this: DOI: 10.1039/x0xx00000x

Nobuhiko Hosono, Anja R. A. Palmans,* and E. W. Meijer*

Received 00th January 2014,
Accepted 00th January 2014

DOI: 10.1039/x0xx00000x

www.rsc.org/

“Soldiers–Sergeant–Soldiers” experiments performed in single-chain polymeric nanoparticles (SCPNs) with an ABA-type triblock architecture carrying chiral and achiral benzene-1,3,5-tricarboxamides (BTAs) in different blocks reveal that the BTAs form segregated, multiple stacks in a single SCPN.

Single-chain polymeric nanoparticles (SCPNs), which are synthetic polymers capable of folding into nanoparticles with covalent/supramolecular interactions, attract considerable interests to mimic biomaterials.[1–3] We have recently developed SCPNs consisting of a synthetic polymer chain with complementary hydrogen-bonding side-groups that can induce a large chain collapse through intramolecular self-assembly providing dynamic crosslinking.[4,5]

Our investigations on SCPNs predominantly focused on systems with ureidopyrimidinone (UPy)[4] and/or benzene-1,3,5-tricarboxyamide (BTA)[5] as the supramolecular crosslinking units. BTA is a well-explored discotic molecule that forms a helical aggregate, stabilized by threefold, lateral hydrogen bonding.[6] The folding behaviour of BTA-based SCPNs has been investigated extensively by our group for facile construction of nanometer-sized objects (Figure 1a), with the ultimate aim to create artificial enzymatic systems.[5b–d] Since a better understanding of the folding process is crucial for tailoring the structure and functions of SCPNs, a quantitative estimation of the extent of folding was attempted by means of model analysis of temperature-dependent circular dichroism (CD) spectra.[5d] However, gathering direct experimental evidence on the internal folding structure still remains challenging since we are neither able to quantify the length of BTA stacks formed in SCPNs nor to distinguish between single and multi-domain present in the folded core. Using a combination of scattering methods, we recently realized that water-soluble BTA-based SCPNs adopt ellipsoidal shapes with an unexpectedly high aspect ratio.[5f] Increasing the degree of polymerization of the SCPN resulted in an increase of the aspect ratio while the cross sectional radius remained constant. As a result, we concluded that the BTA moieties self-assemble into separated, individual stacks providing multiple, folded domains alongside the backbone polymer.[5h]

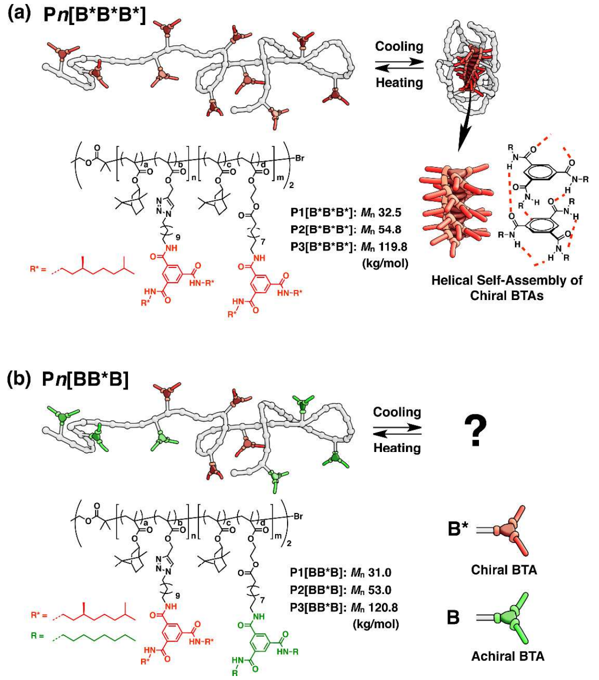

Figure 1. Schematic representations and chemical structures of BTA-based SCPNs. (a) **P*n*[B*B*B*]** and (b) **P*n*[BB*B]** (*n* = 1, 2, and 3).

In SCPNs designed for organic solvents, where the hydrophobic effect is absent, it remained unclear how BTA aggregation occurs and how it affects the global conformation of the polymers.[5a] Here we report intramolecular “Soldiers–Sergeant–Soldiers” (S–S–S) experiments using SCPNs with triblock architectures, as a novel tool to elucidate the folding behavior of SCPNs in organic media. To investigate the extent of supramolecular self-assembly, the S–S–S experiment is a powerful tool that has been applied to a variety of self-assembling motifs including BTAs. In “free” BTA systems (not bounded on a polymer chain), it is known that only 5-mol% of Sergeant BTA, which possesses chiral side chains at the periphery, induces full chiral amplification of the achiral BTA stacks.[6a] This means that one chiral BTA imposes its preferred handedness on twenty achiral BTAs on average. Thus, in a SCPN the S–S–S experiment provides experimental evidence on the possibility of the chiral sergeant to transfer its helical preference to the achiral soldiers.

The chemical structures of S–S–S folding triblock copolymers are depicted in Figure 1b. The ABA-type triblock copolymers were designed to be so-called "Soldier–Sergeant–Soldier" architectures. Sergeants of chiral BTA (**B***) and Soldiers of achiral BTA (**B**) are separately incorporated into the middle (B) and both end (A) blocks, respectively. The subscripts **B** and * denote BTA and the presence of chiral center in the peripheral side chains, respectively. We synthesized the S–S–S triblock copolymers with three different molecular weights ranging from 32 to 120 kg/mol, denoted as **P*n*[BB*B]** (*n* = 1, 2, and 3). The triblock architectures were first realized by two-step atom-transfer radical polymerization (ATRP) in the presence of Cu(I)Br/*N*-butyl-2-pyridylmethanimine catalyst with isobornyl methacrylate and 10 mol% of post-functionalizable comonomers (propargyl methacrylate for the middle block, and hydroxyethyl methacrylate for the both end blocks). The backbone triblock copolymers were functionalized through two consecutive Cu(I)-catalyzed azide-alkyne cycloaddition (CuAAC) for **B*** and ester conjugation reactions for **B**.[5e,†] Sergeant fractions, $f_{\mathbf{B*}}$, are around 37% for all S–S–S copolymers. For comparison, triblock copolymers with all chiral BTAs, denoted as **P*n*[B*B*B*]** (*n* = 1, 2, and 3), were prepared in an identical manner starting with the identical backbone polymers, but now $f_{\mathbf{B*}}$ is 100% (Figure 1a). The characterization data for all triblock copolymers are given in Table 1.

Table 1. Data for Triblock Copolymers.

Polymer	$n_{\mathbf{BTA}}$ in each block[1] [A–B–A]	Total $n_{\mathbf{BTA}}$ /chain	$f_{\mathbf{B*}}$[2]	M_n kg/mol ($Đ$)[3]
P1[BB*B]	[$3.2_{\mathbf{B}} - 3.8_{\mathbf{B*}} - 3.2_{\mathbf{B}}$]	10.2	37%	31.0 (1.20)
P2[BB*B]	[$5.7_{\mathbf{B}} - 6.3_{\mathbf{B*}} - 5.7_{\mathbf{B}}$]	17.7	36%	53.0 (1.42)
P3[BB*B]	[$14.0_{\mathbf{B}} - 16.6_{\mathbf{B*}} - 14.0_{\mathbf{B}}$]	44.6	37%	120.8 (1.56)
P1[B*B*B*]	[$3.2_{\mathbf{B*}} - 3.8_{\mathbf{B*}} - 3.2_{\mathbf{B*}}$]	10.2	100%	32.5 (1.19)
P2[B*B*B*]	[$5.7_{\mathbf{B*}} - 6.3_{\mathbf{B*}} - 5.7_{\mathbf{B*}}$]	17.7	100%	54.8 (1.43)
P3[B*B*B*]	[$14.0_{\mathbf{B*}} - 16.6_{\mathbf{B*}} - 14.0_{\mathbf{B*}}$]	44.6	100%	119.8 (1.70)

[1] Number of chiral (**B***) and achiral BTA (**B**) group determined via ^{1}H NMR with reference to the corresponding numbers determined previously (Figure S1–S3).[5e,†] [2] Sergeant fraction: $n_{\mathbf{B*}}/(n_{\mathbf{B}}+n_{\mathbf{B*}})$. [3] Determined via SEC using THF as the eluent, calibrated with polystyrene standards (Figure S4)[†]. $Đ = M_w/M_n$.

A number of possibilities can be distinguished with respect to how the chiral amplification behavior takes place in the single polymer chain. If full chiral amplification occurs, we expect to observe an identical CD signal intensity between **P*n*[BB*B]** and **P*n*[B*B*B*]** at a fixed BTA concentration. If not, a smaller CD signal of **P*n*[BB*B]** compared to that of **P*n*[B*B*B*]** indicates that the formation of only a single, long BTA stack in the SCPN is no longer realistic, neither with segregated nor intercalated cores (Figure 2a and b). In the latter case, the most likely option is an internal structure that consists of multiple cores, in which communication between **B*** and **B** is restricted in the individual stacks resulting in no or poor chiral amplification (Figure 2c).

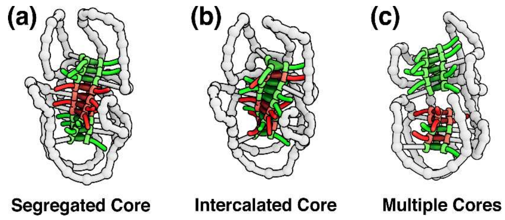

Figure 2. Envisioned folding structures of **P*n*[BB*B]** S–S–S triblock copolymers with chiral BTA (red) and achiral BTA (green). SCPN with (a) segregated and (b) intercalated core, and (c) separated multiple cores.

Temperature-dependent CD measurements using 1,2-dichloroethane (DCE) as a solvent were applied to **P*n*[BB*B]** and **P*n*[B*B*B*]** at the fixed BTA concentration of c_{BTA} = 50 µM (Figure 3). The polymer solutions were heated up to 80 °C, then slowly cooled down to 20 °C at the rate of 1 °C/min to ensure that BTA self-assembly is under thermodynamic control. The CD signal intensity was monitored at 225 nm. Above 60 °C, all of the polymers were CD-silent, indicating that the polymers were molecularly dissolved and adopted unfolded conformations (Figure 3a, c, and e). Upon cooling, a negative Cotton effect was observed for all of the polymers, indicative of the preference for left-handed helical columnar aggregates inside the polymer, which is in accordance with our previous reports.[6] The temperature at which the CD signal starts to appear, T_e (elongation temperature), was 60 °C for all polymers, **P*n*[B*B*B*]** and **P*n*[BB*B]**. This confirms that the same incorporation density of BTAs (10 mol%), either **B** or **B***, was achieved in both polymers, since T_e is dependent on the local concentration of BTA units.[5a]

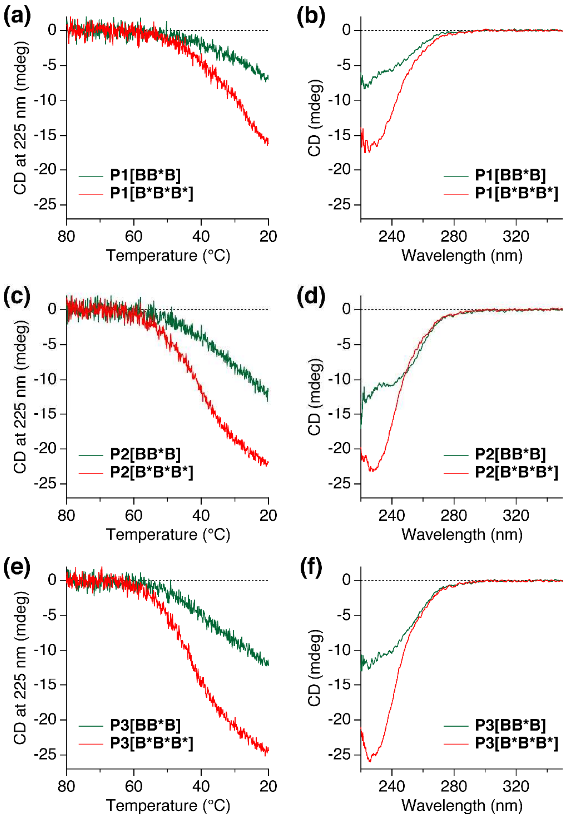

Figure 3. CD cooling curves (a, c, e) and spectra at 20 °C (b, d, f) for **P*n*[BB*B]** (green) and **P*n*[B*B*B*]** (red) (*n* = 1,2, and 3; c_{BTA} = 50 µM in DCE; cooling rate: 1 °C/min). (a, b) **P1** (c, d) **P2**, and (e, f) **P3** series of polymers.

Evaluation of the CD cooling curves shows that the CD signal intensities of all S–S–S polymers **P*n*[BB*B]** never reach the ones of **P*n*[B*B*B*]**, indicating that the chiral amplification is not perfectly operative within the triblock architectures, despite the fact that the local Sergeant fraction, $f_{\mathbf{B*}}$, is high (36–37%) and well above the required 5% for free BTAs. The magnitude of the CD-effects at room temperature on the other hand are higher than the values expected when only chiral BTAs contribute to the CD-effect. As a result, the chiral and achiral BTAs mix, but the perfect polymer conformations represented in Figures 2a,b are highly unlikely. The mixing is also evident from the CD spectral shape of **P*n*[BB*B]**, being different from **P*n*[B*B*B*]** (Figure 3b, d, and f), i.e., double peaks with a maximum at roughly 220 nm and 240 nm, compared to the CD spectrum of the **P*n*[B*B*B*]** with a single peak around 228 nm. In accordance with our previous studies, this differently-shaped CD effect is indicative of an inclusion of achiral BTAs into the helical stacks of the "Sergeant".[6a] This fact suggests the presence of some chiral transfer through *inter*-block communications within **B*** + **B** or the incorporation of **B** in blocks of **B***.

In order to determine in how far the density of the **B** moieties on the polymer backbone affects the incorporation of **B** in blocks of **B*** or *inter*-block communication, we synthesized a series of **P3[BB*B]**-based polymers. In this series we varied the incorporation numbers of **B**, numbered as **P3[–B*–]** ($f_{\mathbf{B*}}$ 100%), **P3[BB*B]a** ($f_{\mathbf{B*}}$ 72%), **P3[BB*B]b** ($f_{\mathbf{B*}}$ 66%), **P3[BB*B]c** ($f_{\mathbf{B*}}$ 62%), and **P3[BB*B]d** ($f_{\mathbf{B*}}$ 45%), where – denotes the absence of any **B** unit in the end blocks.† The incorporation number of **B*** is 16.6 for all polymers, and **B** is 6.4, 8.6, 10.4, and 20.2, respectively. The CD intensity at 225 nm measured at 20 °C after cooling from 80 °C in DCE (c_{BTA} = 50 μM) were plotted for all above polymers as a function of $f_{\mathbf{B*}}$ (Figure 4a). CD spectra and cooling curves for all these polymers are given in Figure S5.† The plot showed a peculiar non-linear dependence on $f_{\mathbf{B*}}$. In particular, **P3[BB*B]** (orange marker) with the highest incorporation density of **B** but the lowest $f_{\mathbf{B*}}$ of 37% showed a stronger signal and exhibited the most pronounced double-peak CD spectrum in this polymer series.† This fact could suggest that the *inter*-block communication starts taking place at a higher incorporation density of **B**.

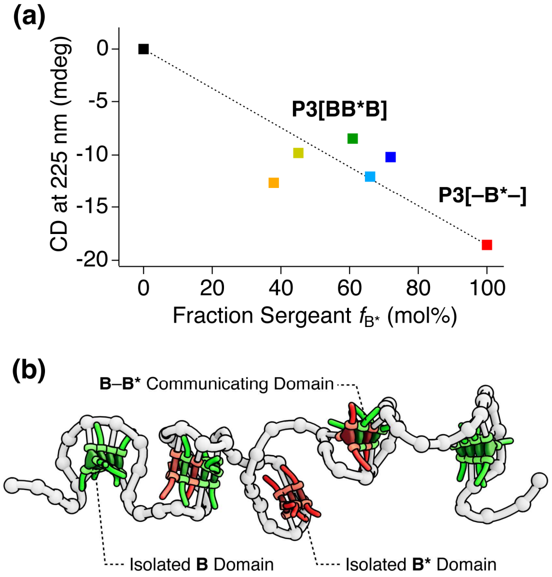

Figure 4. (a) Variable **B** experiment on **P3** series of S–S–S polymers. (c_{BTA} = 50 μM in DCE). **P3[–B*–]** (red), **P3[BB*B]a** (blue), **P3[BB*B]b** (light blue), **P3[BB*B]c** (green), **P3[BB*B]d** (yellow), and **P3[BB*B]** (orange). Imaginary Zero-CD point was plotted with a black marker. (b) Envisioned folding structure of BTA-based S–S–S SCPNs.

Taking all observations into account, we propose a folded structure of BTA-based SCPNs that consists of multiple stacked BTA aggregates (Figure 4b). As a direct result, the organosoluble copolymers are likely to adopt an ellipsoidal, elongated shape, similar to their watersoluble counterparts.[5f] The CD cooling curves of **P1-P3** are almost identical, indicating that the length of the polymers does not affect the melting curves. This observation implies a lack of strong cooperativity in the folding of these polymers.[5h]

In conclusion, we have demonstrated "Sergeant–and–Soldier" experiments in the BTA-based SCPNs with a "Soldier–Sergeant–Soldier" triblock architecture. The results revealed that BTA units incorporated into the polymer chain tend to form segregated, multiple stacks in the SCPNs with some mixing of the BTA-units of the different blocks.

N.H. is thankful to the Japan Society for the Promotion of Science (JSPS) for a Young Scientist Fellowship. This work was supported by the European Research Council (ERC), the Dutch Science Foundation (NWO) and the Dutch Ministry of Education, Culture and Science (Gravity program 024.001.035). ICMS animation studio is acknowledged for the artwork.

Notes and references

Institute for Complex Molecular Systems (ICMS), Eindhoven University of Technology, P.O. Box 513, 5600 MB Eindhoven, The Netherlands. Fax: (+31) 402-451-036. E-mail: a.palmans@tue.nl; e.w.meijer@tue.nl

†Electronic Supplementary Information (ESI) available: Synthesis and characterizations of the polymers. See DOI: 10.1039/c000000x/

1 (a) M. K. Aiertza, I. Odriozola, G. Cabañero, H. –J. Grande and I. Loinaz, *Cell. Mol. Life Sci.*, 2012, **69**, 337; (b) M. Ouchi, N. Badi, J. –F. Lutz, and M. Sawamoto, *Nat. Chem.*, 2011, **3**, 917; (c) O. Altintas and C. Barner-Kowollik, *Macromol. Rapid Commun.*, 2012, **33**, 958.
2 (a) J. B. Beck, K. L. Killops, T. Kang, K. Sivanandan, A. Bayles, M. E. Mackay, K. L. Wooley and C. J. Hawker, *Macromolecules*, 2009, **42**, 5629; (b) B. V. K. J. Schmidt, N. Fechler, J. Falkenhagen and J. –F. Lutz, *Nat. Chem.*, 2011, **3**, 234.
3 (a) E. A. Appel, J. Dyson, J. del Barrio, Z. Walsh and O. A. Scherman, *Angew. Chem. Int. Ed.*, 2012, **51**, 4185; (b) O. Altintas, E. Lejeune, P. Gerstel and C. Barner-Kowollik, *Polym. Chem.*, 2012, **3**, 640; (c) T. Terashima, T. Sugita, K. Fukae, M. Sawamoto, *Macromolecules*, 2014, **47**, 589; (d) J. Romulus, M. Weck, *Macromol. Rapid. Commun.*, 2013, **34**, 1518; (e) D. Chao, X. Jia, B. Tuten, C. Wang, E. B. Berda, *Chem. Commun.*, 2013, **49**, 4178; (f) O. Shishkan, M. Zamfir, M. A. Gauthier, H. G. Börner. J.-F. Lutz, *Chem. Commun.*, 2014, **50**, 1570.
4 (a) E. J. Foster, E. B. Berda and E. W. Meijer, *J. Am. Chem. Soc.*, 2009, **131**, 6964; (b) P. J. M. Stals, M. A. J. Gillissen, R. Nicolaÿ, A. R. A. Palmans and E. W. Meijer, *Polym. Chem.*, 2013, **4**, 2584; (c) P. J. M. Stals, Y. Li, J. Burdyńska, R. Nicolaÿ, A. Nese, A. R. A. Palmans, E. W. Meijer, K. Matyjaszewski and S. S. Sheiko, *J. Am. Chem. Soc.*, 2013, **135**, 11421.
5 (a) T. Mes, R. van der Weegen, A. R. A. Palmans and E. W. Meijer, *Angew. Chem. Int. Ed.*, 2011, **50**, 5085; (b) E. Huerta, P. J. M. Stals, E. W. Meijer and A. R. A. Palmans, *Angew. Chem. Int. Ed.*, 2012, **52**, 2906; (c) M. Artar, T. Terashima, M. Sawamoto, E. W. Meijer and A. R. A. Palmans, *J. Poym. Sci. Part A: Polym. Chem.*, 2014, **52**, 12; (d) T. Terashima, T. Mes, T. F. A. de Greef, M. A. J. Gillissen, P. Besenius, A. R. A. Palmans and E. W. Meijer, *J. Am. Chem. Soc.*, 2011, **133**, 4742; (e) N. Hosono, M. A. J. Gillissen, Y. Li, S. S. Sheiko, A. R. A. Palmans and E. W. Meijer, *J. Am. Chem. Soc.*, 2013, **135**, 501; (f) M. A. J. Gillissen, T. Terashima, E. W. Meijer, A. R. A. Palmans and I. K. Voets, *Macromolecules*, 2013, **46**, 4120; (g) N. Hosono, P. J. M. Stals, A. R. A. Palmans and E. W. Meijer, *Chem. Asian J.*, 2014, **9**, 1099; (h) P. J. M. Stals, M. A. J. Gillissen, T. F. E. Paffen, T. F. A. de Greef, P. Lindner, I. K. Voets, A. R. A. Palmans and E. W. Meijer, *submitted*, 2014.
6 (a) M. M. J. Smulders, P. J. M. Stals, T. Mes, T. F. E. Paffen, A. P. H. J. Schenning, A. R. A. Palmans and E. W. Meijer, *J. Am. Chem. Soc.*, 2010, **132**, 620; (b) Y. Nakano, T. Hirose, P. J. M. Stals, E. W. Meijer

and A. R. A. Palmans, *Chem. Sci.*, 2012, **3**, 148; (c) S. Cantekin, T. F. A. de Greef and A. R. A. Palmans, *Chem. Soc. Rev.*, 2012, **41**, 6125.